Characterization of Pt/γ-Alumina Catalysts Containing Ceria

J. Z. SHYU[1] AND K. OTTO

Research Staff, Ford Motor Company, P. O. Box 2053, Dearborn, Michigan 48121

Effects of adding CeO_2 to platinum on alumina were studied by XPS, XRD, and TPR. Whereas heating of Pt on alumina in air at 800°C results in a surface interactive Pt species having a chemical state of Pt^{+4}, attributed to PtO_2, the same treatment of Pt on CeO_2 or on CeO_2/Al_2O_3 yields a platinum–ceria interactive species with an oxidation state of Pt^{+2}, attributed to PtO. When heated in H_2 at 500°C, Pt on both CeO_2 and CeO_2/Al_2O_3 is completely reduced to Pt^0. Upon reduction in H_2 at 920°C, Pt assists in the formation of $CeAlO_3$. In the reverse reaction, Pt facilitates bulk oxidation of $CeAlO_3$ to CeO_2 at 500°C. © 1989 Academic Press, Inc.

1. INTRODUCTION

In this paper we investigate the chemical states of Pt and ceria on Pt/Al_2O_3 containing ceria under a variety of oxidation and reduction treatments. Ceria (CeO_2) is widely used in automotive catalysts (*1–6*). Recently it has been reported that strong platinum–ceria interaction may have a profound effect on the oxygen storage capacity of ceria (*7, 8*). It is also known that ceria promotes dispersion of Pt (*3, 9–12*), and thus may decrease the rate of alkane oxidation (*9*). However, direct spectroscopic measurements of the oxidation state of Pt on ceria/alumina and structural modifications of Pt by ceria have not yet been reported.

The techniques used in this study are X-ray photoelectron spectroscopy (XPS), X-ray diffraction (XRD), and temperature-programmed reduction (TPR). This investigation is an extension of a similar study on $Pd/CeO_2/Al_2O_3$ (*13*).

2. EXPERIMENTAL SECTION

Samples of CeO_2/Al_2O_3 and $CeAlO_3/Al_2O_3$ are the same used previously (*13*). The CeO_2 sample was prepared by decomposing $(NH_4)_2Ce(NO_3)_6 \cdot 6H_2O$ at 500°C for 4

hr, which resulted in a BET surface area of about 10 m^2/g. Cerium aluminate ($CeAlO_3$) on alumina was prepared by heating 10 wt% CeO_2 on alumina in a flow of 10% hydrogen in argon at 1000°C for 80 hr. The formation of $CeAlO_3$ (with residual Al_2O_3) was confirmed by XRD. Samples that contain Pt were prepared by impregnation of CeO_2, CeO_2/Al_2O_3, and $CeAlO_3/Al_2O_3$ with aqueous solutions of H_2PtCl_6. Platinum foil and PtO_2 powder were obtained from Morton Thiokol, Inc.

Experimental conditions for XPS and XRD have been described previously (*13*). XPS binding energies (BEs) for samples containing alumina and ceria were referenced to Al2*p* at 74.5 eV and O1*s* at 529.0 eV, respectively. Reduction was carried out in flowing H_2 in a reactor attachment (Perkin Elmer Company) of the XPS spectrometer. The reactor can be operated at a maximum temperature of 600°C. Therefore, reduction at higher temperatures had to be carried out in a separate quartz-glass reactor. As a result, such samples were exposed to air while they were transferred to the reactor attachment for further treatment. An Altamira system was used for TPR experiments. A reducing mixture of 10% H_2/Ar was kept at a flow rate of 30 cm^3/min. The heating rate was 15°C/min.

The basis for estimating the relative

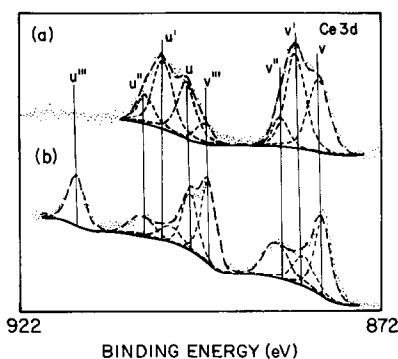[1] Current address: Amoco Research Center, Building 600, Naperville, IL 60566.

FIG. 1. Ce3d XPS spectra of (a) 7% CeAlO₃/Al₂O₃, (b) CeO₂.

amount of Ce^{+4} in the total Ce3d XPS spectra has been explained in a companion paper (13). For the reader's convenience, the illustrations are repeated here. Figure 1 shows the Ce3d spectra of CeO_2 and 7% $CeAlO_3/Al_2O_3$, which consist of 100% Ce^{+4} and 100% Ce^{+3}, respectively. If one assumes a uniform mixture of Ce^{+3} and Ce^{+4}, a series of Ce3d spectra can be synthesized mathematically by a linear combination of the peak area-normalized Ce3d spectra of CeO_2 and $CeAlO_3$. A plot of the % u''' in these synthesized spectra as a function of % CeO_2 is shown in Fig. 2. The dashed line in Fig. 2 is obtained by a least-squares fit of the data points through the origin, whereas the solid line is a direct connection between two end points. The dashed curve in Fig. 2 is the correlation curve used to translate the % u''' in the Ce3d region into % CeO_2 in the catalyst samples.

3. RESULTS AND DISCUSSION

3.1. XPS and XRD Analysis

3.1.1. Pt/Al₂O₃ and Pt/CeO₂. The Pt phase is examined first. Analysis by XRD of 10 wt% Pt on alumina, calcined at 800°C, revealed metallic platinum only. After this calcination, XPS did not detect any chlorine derived from the H_2PtCl_6 used for the Pt deposition. The influence of chlorine on the chemical state of Pt is therefore deemed to be unimportant in this work. Oxides of

platinum were absent in the XRD spectrum, as particles of Pt oxides are decomposed above 500°C. On ceria at a loading of 5 wt% no Pt phase was detected after the same calcination procedure, indicating that the Pt particles were too small to produce distinct XRD lines.

Information on the Pt surface state was obtained by XPS. The Pt4d lines were measured in addition to the Pt4f lines, since the latter overlap with the Al2p line of Al_2O_3. The Pt4f7/2 and Pt4d5/2 BEs of commercial Pt^0 and PtO_2 samples were measured for comparison. They are in good agreement with literature values (*14–17*). The BEs for PtO were taken from the literature (*14–17*).

Pt4f and Pt4d XPS spectra of 10 wt% Pt/ Al_2O_3 and 5 wt% Pt/CeO_2 after calcination at 800°C are shown in Fig. 3. The Pt4f7/2 BEs were obtained from these spectra by a least-squares fit, assuming a constant separation of 3.4 eV and a constant ratio of 0.75 between Pt4f5/2 and Pt4f7/2 lines. These calculated BEs are also listed in Table 1. The sample containing 10 wt% Pt on Al_2O_3 yields Pt4f7/2 and Pt4d5/2 BEs, respectively, at 74.8 and 317.0 eV, characteristic for Pt^{+4}, which is tentatively assigned to PtO_2. The 5 wt% Pt/CeO_2 sample shows the characteristic BEs of Pt^{+2}, attributed to PtO, both in the regions of Pt4f7/2 (72.5 eV) and Pt4d5/2 (315.3 eV). At 500°C, hydrogen reduces the Pt species on both Al_2O_3
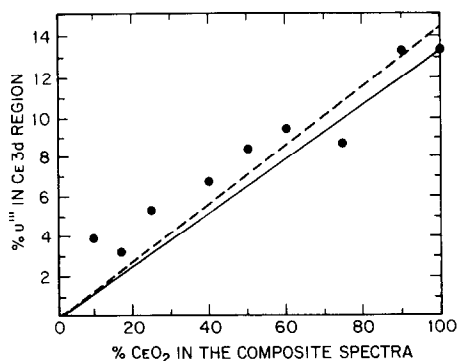

FIG. 2. Correlation of % u''' in synthesized spectra with respect to % CeO_2 in the Ce3d spectra.
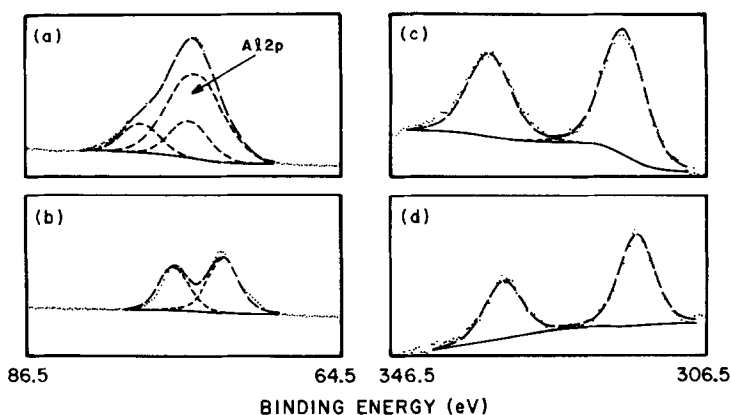
FIG. 3. Pt4f and Pt4d XPS spectra after calcination at 800°C: (a) and (c) 10 wt% Pt/Al$_2$O$_3$ (b) and (d) 5 wt% Pt/CeO$_2$.

and CeO$_2$ completely to Pt^0, as evidenced by the Pt4f7/2 and Pt4d5/2 BEs shown in Table 1.

Since under these experimental conditions on alumina only particles of metallic Pt are detected by XRD, the presence of Pt^{+4} (PtO$_2$) suggests that XPS identifies a surface and/or amorphous Pt species associated with dispersed phase platinum in a PtO$_2$–Al$_2$O$_3$ complex (18–20). Because the metallic Pt is present mainly in the bulk, its contribution is not clearly resolved by XPS. On ceria, however, the fact that no Pt phase was detected by XRD suggests that all of

the platinum is finely dispersed as a result of Pt–CeO$_2$ interaction.

3.1.2. Pt–CeO$_2$/Al$_2$O$_3$. XPS spectra of Pt4f's and Pt4d's for 10 wt% Pt/Al$_2$O$_3$ containing 20 wt% CeO$_2$ are summarized in Table 2 and Fig. 4. After calcination at 800°C, Pt gives a BE of Pt4f7/2 at 72.4 eV and a BE of Pt4d5/2 at 315.2 eV, characteristic of Pt^{+2} (PtO). The absence of the Pt^{+4} BEs suggests that surface Pt preferentially interacts with CeO$_2$, since surface Pt in Pt/Al$_2$O$_3$ after the same calcination yields the characteristic BEs of PtO$_2$, as mentioned earlier. The TPR results, given below, support this concept more convincingly. As expected, reduction by H$_2$ at 500°C results in the BE of Pt^0 in both the Pt4f7/2 and Pt4d5/2 regions.

Exposure to hydrogen at higher temperatures, however, produces a profound change in the Pt state. A sample of 10 wt% Pt/alumina containing 20 wt% CeO$_2$ was reduced at 920°C and then exposed to ambient air. The Pt state of this sample is characterized by a Pt4f7/2 BE of 72.9 eV which is slightly higher than that of PtO (Table 1). After this thermal pretreatment, exposure of the sample to H$_2$ at 500°C does not reduce the Pt to its metallic state, shown by the Pt spectra in Figs. 4b and d. In these XPS spectra, Pt gives a Pt4f7/2 BE of ≈72.1 eV and a Pt4d5/2 BE of 315.0 eV,

TABLE I

XPS Data of Reference Pt Compounds, Pt/Al$_2$O$_3$ and Pt/CeO$_2$

Sample	Treatment history	BE (eV)^a		Assignment
		Pt4f7/2	Pt4d5/2	
Pt foil	Sputtered clean	71.2	314.0	Pt^0
PtO	From literature^b	72.6	315.3	PtO
PtO$_2$	As received	74.2	317.0	PtO$_2$
10% Pt/Al$_2$O$_3$	1. 800°C calcined	74.8	317.0	PtO$_2$
	2. 500°C reduced	71.2	314.2	Pt^0
5% Pt/CeO$_2$	1. 800°C calcined	72.5	315.3	PtO
	2. 500°C reduced	71.1	314.1	Pt^0

^{a} BEs were referenced to Al2p at 74.5 eV, and O1s at 529.0 eV, respectively, for alumina- and ceria-supported Pt.
^{b} Taken from literature, as indicated in the text.

TABLE 2

XPS Data for CeO_2/Al_2O_3 Containing Pt

Sample	Treatment history	BE (eV)[a]		Assignment[b]		
		Pt4f7/2	Pt4d5/2	% u'''	% CeO_2[c]	Pt
10% Pt,20% CeO$_2$	1. 800°C calcined	72.4	315.2	9.9	69	PtO
	2. 500°C reduced	71.3	313.9	10.0	70	Pt^0
	3. 920°C reduced/A^d	72.9	—	0.0	0	
	a. Above, 500°C reduced	72.1	315.0	0.0	0	PtCeO$_x$
	b. Above, 500°C calcined	72.3	—	9.4	66	PtO
10% Pt,10% CeAlO$_3$	1. 500°C calcined	72.6	—	9.2	65	PtO
	2. 920°C reduced	—	—	0.0	0	

[a] BEs were referenced to Al2p line at 74.5 eV.

[b] Assignment of the Pt species is based on BEs Pt4f7/2 and Pt4d5/2.

[c] Numbers represent % CeO_2 in the Ce3d spectra, based on the method described in Ref. (13).

[d] /A denotes that samples have been exposed to air at room temperature before analysis.

values which are substantially higher than the corresponding BEs for Pt^0 (71.2 and 314.0 eV, respectively). The yet unidentified Pt species is tentatively assigned to a surface Pt–CeO$_x$/Al$_2$O$_3$ complex formed during high-temperature reduction (12). This complex formation may cause a BE shift, resulting from hybridization and valence mixing of Pt and Ce4f valence orbitals (21–22).

The chemical change in cerium caused by reduction in H$_2$ at 920°C is also apparent from the XPS spectra in the Ce3d region (Fig. 5). Calcination at 800°C results in a Ce species having a % u''' that amounts to ≈9.9% in the total Ce3d region (Fig. 5a). Based on the correlation scheme (13) (cf. Figs. 1 and 2) the % u''' is equivalent to ≈69% CeO$_2$ (and ≈31% Ce^{+3}) in the sample. Reduction at 920°C, followed by expo-
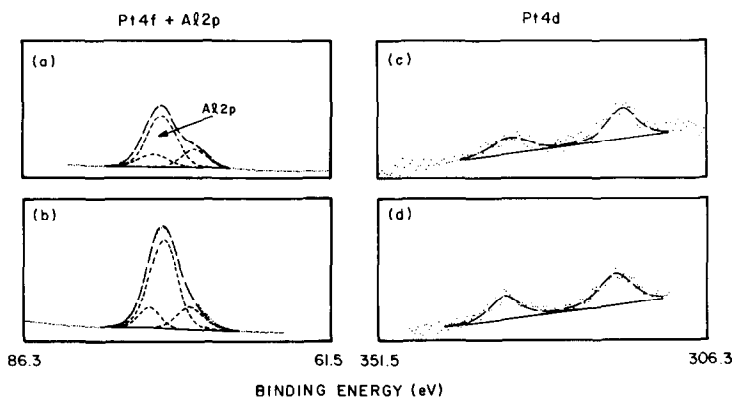

BINDING ENERGY (eV)

FIG. 4. Pt4f and Pt4d XPS spectra of Pt/CeO$_2$/Al$_2$O$_3$: (a) 10 wt% Pt + 20 wt% CeO$_2$, reduced *in situ* at 500°C, (b) 10 wt% Pt + 20 wt% CeO$_2$/Al$_2$O$_3$, reduced at 920°C and exposed to ambient air, (c) 10 wt% Pt + 20 wt% CeO$_2$/Al$_2$O$_3$, reduced *in situ* at 500°C, (d) sample (b) reduced *in situ* at 500°C.
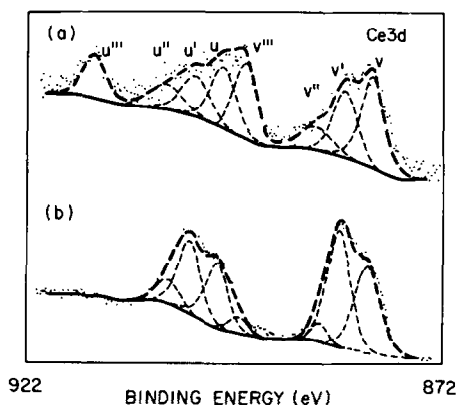
sure to ambient air, results in a disappearance of the u''' peak (Fig. 5b), indicating complete reduction of Ce^{+4} to Ce^{+3}. It should be noted that the conversion to Ce^{+3} is catalyzed by platinum. Without platinum only a partial reduction ($\approx70\%$) was achieved at 920°C (13, 23).

The XPS data describing the state of cerium and platinum in the system Pt/CeO₂/Al₂O₃ under different conditions are summarized in Table 2. Calcination at 800°C results in CeO₂ and PtO (Pt^{+2}). Reduction at 500°C leaves the CeO₂ essentially unchanged according to the % u''' in the Ce3d spectrum, while Pt is reduced to Pt^0. During reduction at 920°C, Ce^{+3} species are formed which retain their oxidation state even after exposure to ambient air. The results are in agreement with literature data, based on thermodynamic, XPS, and kinetic analyses (23–28). At the same time, the surface Pt remains in an oxidized state, even after reduction at 500°C.

Structural changes of ceria during reduction at 920°C were also investigated by XRD. As shown in Fig. 6b, the Ce^{+3} species obtained upon reduction at 920°C is primarily attributable to CeAlO₃ (13, 23). The sample calcined at 800°C (Fig. 6a) consists mainly of Pt^0, CeO₂, and γ-Al₂O₃, whereas the sample reduced at 920°C contains Pt^0, CeAlO₃, and γ-Al₂O₃. No Ce₂O₃ was de-

tected in the reduced sample, as it is oxidized completely to CeO₂ when exposed to air (21–23). It should be noted that XRD gives no indication of formation of the Pt–CeO$_x$/Al₂O₃ complex, suggesting that the complex implied by the XPS data, if it exists, is present on the surface only, unless it has an amorphous structure.

The reversibility of CeAlO₃ formation was further investigated by synthesizing bulk aluminate from γ-alumina impregnated by an aqueous cerium nitrate solution and heating in H₂ to 1000°C (23). This sample, containing 10 wt% CeAlO₃ on Al₂O₃, was impregnated by an aqueous solution of H₂PtCl₆, resulting in a Pt loading of 10 wt%. XPS analysis of the u''' peak in the Ce3d region indicated that, after calcination at 500°C, approximately 65% of the cerium was in the form of CeO₂ (Table 2). At the same time, the platinum species shows a Pt4f7/2 BE of ≈72.6 eV which is close to that of PtO. The formation of the CeO₂ phase with residual CeAlO₃ after the calcination is confirmed by XRD. Without Pt, the temperature has to be increased to at
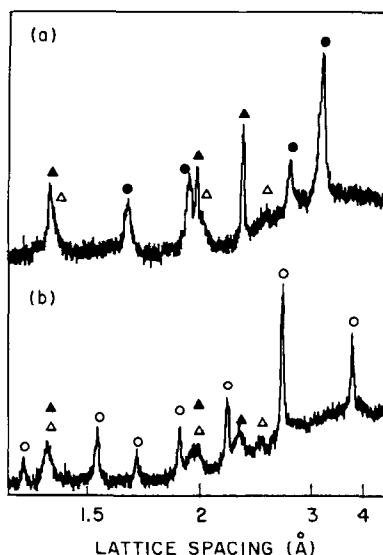

FIG. 6. X-ray powder diffraction pattern of 1 wt% Pt on 20 wt% CeO₂/Al₂O₃: (a) after calcination at 800°C, (b) and reduction at 920°C(b); (△): γ-alumina, (●): CeO₂, (○): CeAlO₃, (▲): Pt^0.
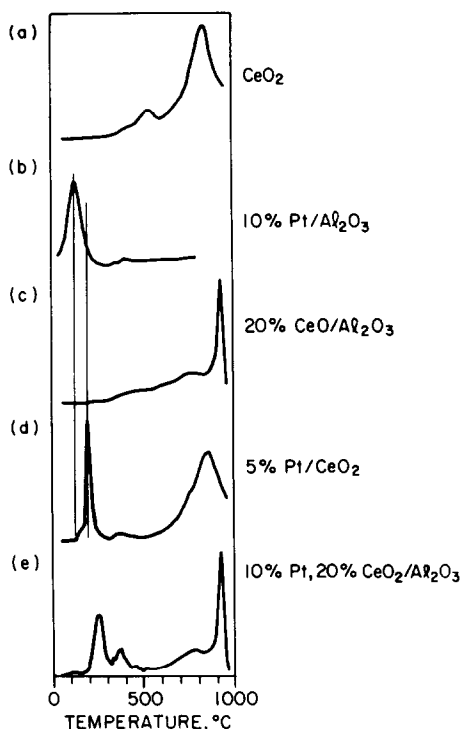
FIG. 7. TPR profiles of the system Pt/CeO₂/γ–alumina.

least 800°C in order to oxidize CeAlO₃ to CeO₂ (13, 23, 25). It is thus apparent that the presence of Pt facilitates the oxidation of CeAlO₃. The CeAlO₃ phase is completely restored by reduction at 920°C, as indicated by XRD and by the disappearance of the u‴ peak in the Ce3d region (Table 2).

3.2. TPR Analysis

The TPR profiles of the system Pt/CeO₂/Al₂O₃ are rather complex. The data are, however, qualitatively useful as supportive evidence for some of the component interactions. The TPR profile for CeO₂ in Fig. 7a shows two major peaks at approximately 580, and above 800°C, and a minor peak at about 450°C. The peak at 450°C is due to removal of surface oxygen (1), and the peaks at 580°C and above 800°C are attributed, respectively, to formation of nonstoichiometric cerium oxides and of Ce₂O₃ (23).

Since a Pt loading of 10 wt% on Al₂O₃ exceeds the saturation concentration of fully dispersed Pt (≈5 wt%), platinum in the particulate phase should be present. However, calcination at 800°C would have decomposed the particulate phase of Pt oxides to bulk Pt⁰, which cannot give any TPR signal. The major peak for 10% Pt/Al₂O₃ at ≈130°C (Fig. 7b) is attributed to dispersed Pt on alumina (PtO₂–Al₂O₃ complex), coexisting with bulk Pt⁰. This peak is known to move toward higher temperature as the Pt concentration decreases and approaches eventually ≈400°C at very low Pt loadings (27). The small peak at ≈400°C is attributed to a residue of the dispersed phase Pt in isolated patches.

A TPR profile for 20 wt% CeO₂/Al₂O₃ is shown in Fig. 7c. This ceria loading exceeds greatly monolayer coverage on alumina (≈6 wt%) (1, 23), therefore, particulate and dispersed phases of CeO₂ should coexist. The sample shows four poorly resolved peaks at approximately 400, 600, 750°C, and a sharp peak above 800°C. These peaks are attributed to removal of surface oxygen from ceria, formation of nonstoichiometric cerium oxides from CeO₂, formation of CeAlO₃ from dispersed ceria on alumina, and formation of Ce₂O₃, respectively (23). The TPR profile for 5% Pt/CeO₂ (Fig. 7d) shows clearly the main peak of CeO₂ above 800°C (cf. Fig. 7a). The peak assigned to the formation of nonstoichiometric cerium oxides (normally around 580–600°C) is not evident in the profile. The suppression of this peak is possibly a result of interaction between Pt and ceria. The peak at ≈200°C in the TPR profile (Fig. 7d) is considered to result from such an interaction between Pt and ceria. Compared with 10% Pt/Al₂O₃, Pt on ceria has a higher reduction temperature than given by the primary Pt peak on alumina (≈130°C).

A TPR profile of the ternary system, 10 wt% Pt/Al₂O₃ containing 20 wt% CeO₂, is shown in Fig. 7e. The 240°C peak is, within experimental error, characteristic of the Pt–CeO₂ interactive species (cf. Fig. 7d),
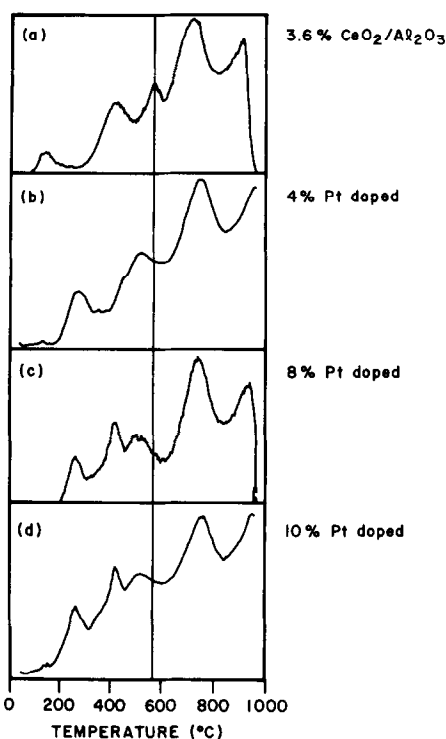
FIG. 8. TPR profiles of 3.6 wt% CeO$_2$/Al$_2$O$_3$ containing Pt.

whereas the peak at ≈400°C is deemed to originate from a small amount of dispersed Pt associated with alumina (27). Also, as shown in Fig. 7e, peaks assigned to the formation of CeAlO$_3$ from the dispersed ceria (at ≈750°C) and Ce$_2$O$_3$ from CeO$_2$ (above 900°C) are present. The absence of a peak around 130°C is taken as evidence that Pt on Al$_2$O$_3$ is present exclusively in the dispersed phase. It should be noted that the Pt–CeO$_2$ interactive species is the predominant species observed by XPS, while the PtO$_2$–Al$_2$O$_3$ complex is not resolvable probably because of low abundance.

To examine the influence of platinum concentration on the interaction between Pt and ceria, TPR experiments were carried out with 3.6 wt% CeO$_2$/Al$_2$O$_3$ containing varying amounts of Pt. As shown in Fig. 8a, 3.6% CeO$_2$/Al$_2$O$_3$ without Pt is described by five TPR peaks. The peak at ≈100°C is probably associated with adsorbed oxygen on alumina (1). The other four peak positions are consistent with those observed for 20% CeO$_2$/Al$_2$O$_3$ (cf. Fig. 7c). Because of the relatively low concentration of particulate phase ceria, the intensity of the peak assigned to the formation of Ce$_2$O$_3$ (above 800°C) is relatively low compared to the peak associated with the formation of CeAlO$_3$ (at ≈760°C).

When 4% Pt was added to 3.6% CeO$_2$/ Al$_2$O$_3$, which corresponds to a Pt : CeO$_2$ atomic ratio of approximately 1 : 1, an additional peak emerged at ≈250°C (Fig. 8b) which corresponds to the reduction temperature of Pt in 10% Pt/20% CeO$_2$/Al$_2$O$_3$ (Fig. 7e). A small peak around 450°C is present which has previously been assigned to removal of surface oxygen of ceria on alumina.

A concentration of 3.6 wt% CeO$_2$ is able to cover only a small fraction of the alumina support. Since Pt–CeO$_2$ interaction is already evident at a loading of 4 wt% Pt, it is apparent that Pt interacts preferentially with ceria in the presence of a much larger alumina surface. As the Pt concentration is increased to 8 and 10 wt% (Fig. 8c and d) the ceria surface becomes saturated. Additional Pt then occupies the alumina surface. Thus, a new peak at ≈420°C, characteristic of dispersed Pt on alumina, emerges at higher Pt loadings. The species attributed to coexistence of both the dispersed and particulate phases of platinum on alumina (≈130°C in Fig. 7c) is not detected by TPR in any of these samples containing up to 10 wt% Pt. It thus appears that addition of ceria facilitates Pt dispersion, in agreement with the literature (3, 7–9, 27).

4. CONCLUDING REMARKS

The experimental results in this paper can be summarized as follows:

(1) A strong interaction between Pt and CeO$_2$ under oxidizing conditions at 800°C results in formation of Pt^{+2} in the surface, attributed to PtO. Under the same conditions, surface Pt on alumina is present in a PtO$_2$–Al$_2$O$_3$ complex. When both ceria and

alumina are present, Pt interacts preferentially with ceria.

(2) Upon reduction in H_2 at 920°C, Pt assists in the formation of $CeAlO_3$ from CeO_2/Al_2O_3, while Pt on the surface is possibly associated with Ce^{+3} in a $Pt–CeO_x$ surface complex.

(3) At 500°C, Pt facilitates the bulk oxidation of $CeAlO_3/Al_2O_3$ to CeO_2/Al_2O_3, whereas Pt is oxidized to Pt^{+2} (PtO).

Based on these observations, it is clear that Pt and cerium oxides are subject to mutual interaction. This interaction facilitates a reversible formation of $CeAlO_3$ and improves dispersion of Pt.

It is of interest to compare the results for $Pt/CeO_2/Al_2O_3$ reported here and for $Pd/CeO_2/Al_2O_3$, described in a companion paper (13). It was found that the interaction between Pt and CeO_2 is intrinsically much stronger than that between Pd and CeO_2. Both Pt and Pd assist in the formation of bulk $CeAlO_3$ upon reduction at 920°C from CeO_2/Al_2O_3. However, while Pd is reduced to its metallic state without appreciable interaction with cerium, Pt becomes stabilized as a surface complex. In the reverse reaction, metallic Pd dissociates O_2 in ambient air, which results in surface oxidation of $CeAlO_3$ to CeO_2. The interaction of Pt and cerium makes it necessary to heat $Pt/CeO_2/Al_2O_3$ to a higher temperature (500°C) to accomplish the $CeAlO_3$ oxidation.

REFERENCES

1. Yao, H. C., and Yu-Yao, Y. F., *J. Catal.* **86,** 254 (1984).
2. Gandhi, H. S., Piken, A. G., Shelef, M., and Delosh, R. G., SAE Paper No. 760201, Warrendale, PA, 1976.
3. Yao, H. C., *Appl. Surf. Sci.* **19,** 398 (1984).
4. Yu-Yao, Y. F., and Kummer, J. T., *J. Catal.* **106,** 307 (1987).
5. Su, E. C., and Rothschild, W. G., *J. Catal.* **99,** 506 (1986).
6. Su, E. C., Montreuil, C. N., and Rothschild, W. G., *Appl. Catal.* **17,** 75 (1985).
7. Metcalf, I. S., and Sundaresan, S., *Chem. Eng. Sci.* **41,** 1109 (1986).
8. Jin, T., Okuhara, T., Mains, G. J., and White, J. M., *J. Phys. Chem.* **91,** 3310 (1987).
9. Gandhi, H. S., and Shelef, M., in "Catalysis and Automotive Pollution Control" (A. Crucq and A. Frennet, Eds.), p. 199. Elsevier, Amsterdam, 1987.
10. Yu-Yao, Y. F., *Ind. Eng. Chem. Prod. Res. Dev.* **19,** 293 (1980).
11. Kummer, J. T., *J. Phys. Chem.* **90,** 4747 (1986).
12. Summer, J. C., and Ausen, S. A., *J. Catal.* **58,** 131 (1979).
13. Shyu, J. Z., Otto, K., Watkins, W. L. H., Gandhi, H. S., Graham, G. W., and Belitz, R. K., *J. Catal.* **114,** 23 (1988).
14. Vedrine, J. C., Duflux, M., Naccache, C., and Imelik, B., *J. Chem. Soc. Faraday Trans. 1* **74,** 440 (1978).
15. Gentry, S. J., Hurst, N. W., and Jones, A., *J. Chem. Soc. Faraday Trans 1* **77,** 603 (1981).
16. Bancroft, G. M., Adams, I., Coatsworth, L. L., Bennewitz, C. D., Brown, J. D., and Westwood, W. D., *Anal. Chem.* **47,** 586 (1975).
17. Kim, K. S., Winograd, N., and Davis, R. E., *J. Amer. Chem. Soc.* **93,** 6296 (1971).
18. Yao, H. C., Sieg, M., and Plummer, H. K., Jr., *J. Catal.* **59,** 365 (1979).
19. Johnson, M. F. L., and Keith, C. D., *J. Phys. Chem.* **67,** 200 (1963).
20. Hermann, R. A., Alder, S. F., Goldstein, M. S., and Debaun, R. M., *J. Phys. Chem.* **65,** 2189 (1961).
21. Fuggle, J. C., *J. Less-Common Met.* **93,** 159 (1983).
22. Fuggle, J. C., Hillebrecht, F. U., Zolnierek, Z., and Lasser, R., *Phys. Rev. B* **27,** 7330 (1983).
23. Shyu, J. Z., Weber, W. H., and Gandhi, H. S., *J. Phys. Chem.*, in press.
24. Rosynek, M. P., *Catal. Rev. Sci. Eng.* **16,** 111 (1977).
25. Mizuno, M., Berjoan, R., Coutures, J. P., and Feox, M., *Yagyo-Kyokai-Shi* **83,** 50 (1975).
26. Yamaguchi, T., Ikeda, N., Hattori, H., and Tanabe, K., *J. Catal.* **67,** 324 (1981).
27. Yao, H. C., Gandhi, H. S., and Shelef, M., in "Metal–Support and Metal Additive Effects in Catalysis" (B. Imelik, Ed.), p. 159. Elsevier, Amsterdam, 1982.
28. Kaufherr, N., Mendelocivi, L., and Steinberg, M., *J. Less-Common Met.* **107,** 281 (1985).